



**HAL**  
open science

## Sororin pre-mRNA splicing is required for proper sister chromatid cohesion in human cells.

Erwan Watrin, Maria Demidova, Tanguy Watrin, Zheng Hu, Claude Prigent

► **To cite this version:**

Erwan Watrin, Maria Demidova, Tanguy Watrin, Zheng Hu, Claude Prigent. Sororin pre-mRNA splicing is required for proper sister chromatid cohesion in human cells.. EMBO Reports, 2014, 15 (9), pp.948-955. 10.15252/embr.201438640 . inserm-01057472

**HAL Id: inserm-01057472**

**<https://inserm.hal.science/inserm-01057472>**

Submitted on 22 Aug 2014

**HAL** is a multi-disciplinary open access archive for the deposit and dissemination of scientific research documents, whether they are published or not. The documents may come from teaching and research institutions in France or abroad, or from public or private research centers.

L'archive ouverte pluridisciplinaire **HAL**, est destinée au dépôt et à la diffusion de documents scientifiques de niveau recherche, publiés ou non, émanant des établissements d'enseignement et de recherche français ou étrangers, des laboratoires publics ou privés.

**Sororin pre-mRNA splicing is required  
for proper sister chromatid cohesion in human cells**

Erwan Watrin<sup>1,2,\*</sup>, Maria Demidova<sup>1,2</sup>, Tanguy Watrin<sup>1,2</sup>, Zheng Hu<sup>1,2</sup> and Claude Prigent<sup>1,2</sup>.

<sup>1</sup> Centre National de la Recherche Scientifique, UMR 6290, Rennes, 35000, France.

<sup>2</sup> Université de Rennes 1, Institut de Génétique et Développement de Rennes, Rennes, France.

Running title: Spliceosome regulates sister chromatid cohesion through sororin

Keywords: Prp19 complex, sister chromatid cohesion, sororin, pre-mRNA maturation, genome stability

\* Corresponding author: erwan.watrin@univ-rennes1.fr

Phone: +33 (0) 2 23 23 43 32; Institut de Génétique et Développement, UMR6290 CNRS-Université de Rennes 1, 2 avenue Pr Léon Bernard, CS 34317, F-35043 Rennes Cedex, France.

Word count : 34,446 characters

## **Summary**

Sister chromatid cohesion, which depends on cohesin, is essential for the faithful segregation of replicated chromosomes. Here, we report that splicing complex Prp19 is essential for cohesion in both G2 and mitosis, and consequently for the proper progression of the cell through mitosis. Inactivation of splicing factors SF3a120 and U2AF65 induces similar cohesion defects to Prp19 complex inactivation. Our data indicate that these splicing factors are all required for the accumulation of cohesion factor sororin, by facilitating the proper splicing of its pre-mRNA. Finally, we show that ectopic expression of sororin corrects defective cohesion caused by Prp19 complex inactivation. We propose that the Prp19 complex and the splicing machinery contribute to the establishment of cohesion by promoting sororin accumulation during S phase, and are, therefore, essential to the maintenance of genome stability.

## Introduction

In eukaryotes, sister chromatid cohesion (SCC) is essential for faithful transmission of the replicated genome between generations and depends on cohesin (Guacci et al., 1997; Losada et al., 1998; Michaelis et al., 1997). In vertebrates, cohesin is composed of the core subunits Smc1, Smc3, Scc1 and SA1 or SA2 (Losada et al., 2000; Sumara et al., 2000), and the regulatory proteins Pds5A or Pds5B (Gandhi et al., 2006; Kueng et al., 2006; Losada et al., 2005; Schmitz et al., 2007; Sumara et al., 2000), Wapl (Gandhi et al., 2006; Kueng et al.) and sororin (Rankin et al., 2005). Establishment of SCC in S phase requires acetylation of Smc3 by Esco1 and Esco2 on two lysine residues at positions 105 and 106 in humans (Nishiyama et al., 2010; Rolef Ben-Shahar et al., 2008; Unal et al., 2008; Zhang et al., 2008). As cells progress in S phase, newly synthesised sororin binds to acetylated Smc3, counteracts the anti-cohesive property of Wapl and promotes SCC establishment (Nishiyama et al., 2010; Ouyang et al., 2013).

The Prp19 complex is composed of four core proteins: Prp19, Cdc5L, Plrg1 and Spf27/BCAS2, and of three associated proteins CTNNBL1, AD002 and HSP73 (Ajuh et al., 2000; Grote et al., 2010). Prp19 complex functions in pre-mRNA splicing (Cheng et al., 1993; Tarn et al., 1993), in DNA damage response (Zhang et al., 2009) and in transcription elongation (Chanarat et al., 2011). Inactivation of Prp19 complex by RNAi causes cell's arrest in prometaphase with misaligned chromosomes (Hofmann et al., ; Neumann et al., 2010), similar to cellular consequences of SCC deficiency. Furthermore, Prp19 complex and cohesin were described as being part of a large and evolutionarily conserved protein complex (McCracken et al., 2005). Based on these observations, we hypothesised that Prp19 complex may be involved in the regulation of SCC in human.

## Results and Discussion

### Prp19 complex is required for sister chromatid cohesion in mitosis

To address whether Prp19 complex functions in SCC, we investigated consequences of depleting Prp19 complex core components on mitotic SCC and on progression through mitosis in HeLa cells. To assess phenotype specificity, we used a HeLa cell line that constitutively expresses murine Cdc5L fused to a localisation-and-affinity-purification (LAP) tag containing green fluorescent protein (GFP) (Figure E1A-B,D) and resistant to hCdc5L siRNAs (Figures 1D and E1C). Cells were transfected with control, Scc1, Cdc5L or Prp19 small interfering RNAs (siRNAs) and we analysed SCC status in mitoses 24, 48 and 72 hours later, by observation of spread chromosomes (Figure 1A). In both cell lines, most of control cells displayed normal cohesion when a separation of sister chromatids 72 hours after transfection was observed in up to 90 % of cells depleted of Cdc5L or Prp19, similar to depletion of cohesin itself (Figure 1B, C). Consistently, most of mCdc5L-LAP cells depleted of Scc1 and Prp19 displayed cohesion defects (Figure 1C). By contrast, Cdc5L depletion had almost no effect on SCC in these cells, demonstrating that reduced level of endogenous Cdc5L protein caused SCC defects. Western blot analyses revealed that total amounts of Prp19 and Cdc5L were reduced respectively in Cdc5L and in Prp19 depleted cells (Figure 1D), possibly because one becomes unstable in the absence of the other. Consistent with the cohesion defects in mitosis, inactivation of Prp19 complex resulted in an arrest in prometaphase, with the chromosomes failing to align on the metaphase plate (Figure E1E-G). Importantly, in these cells enrichment of the centromeric region in the chromosome passenger protein Aurora B was maintained (Figure 1E), demonstrating that cohesion loss was not due to an

untimely cell's entry into anaphase. Thus, the depletion of either Cdc5L or Prp19 leads to the premature separation of sister chromatids implying that Prp19 complex is required for normal SCC in mitosis. We also noticed that Cdc5L and Prp19 depleted cells displayed aberrant, collapsed mitotic spindles (Figure E1E and F) that were more pronounced in Cdc5L than in Prp19 depleted cells, presumably because of differences in depletion efficiency. The appearance of these abnormal spindles is unlikely to be an indirect consequence of defective SCC, as this was not observed in Scc1 depleted cells. Rather, it could indicate a distinct and specific role of Prp19 complex in mitotic spindle assembly, as reported recently (Hofmann et al., 2013).

**Prp19 complex is required for accumulation of sororin protein through splicing of *sororin* pre-mRNA and for interphase cohesion**

As Prp19 complex functions in pre-mRNA splicing, its inactivation may affect splicing of pre-mRNA(s) encoding protein(s) essential to SCC and thus induce cohesion defects in an indirect manner. Consistent with this possibility we observed that depletion of two splicing factors distinct from Prp19 complex, SF3A120 and U2AF65 (Hoffman and Grabowski, 1992; Tanackovic and Kramer, 2005), as well as chemical inhibition of splicing using spliceostatin A (SSA, Kaida et al., 2007) also triggered defective mitotic cohesion (Figure 2A-B). These treatments also increased mitotic indices, except for SF3A120 depletion where only few cells were in mitosis possibly because additional role of SF3A120 (Figure 2C). This indicates that SCC defects are common early consequence of splicing deficiency, and suggests that Prp19 complex involvement in SCC is an indirect consequence of its function in splicing. If true, Prp19 complex inactivation should then affect the production of protein(s) required for normal cohesion. To test this possibility we analysed cellular levels of known proteins

involved in cohesion after Prp19 complex inactivation. HeLa cells treated with control, Cdc5L or Prp19 siRNAs were synchronised at the G1/S transition by double thymidine arrest. Before the second release and 4 hours later, total protein extracts were prepared and analysed by western blotting experiments (Figure 3A). In control cells, level of sororin, which is essential to SCC (Rankin et al., 2005; Schmitz et al., 2007), increased during the course of the experiment, consistent with its accumulation during S phase (Nishiyama et al., 2010), and similar to the accumulation of its mRNA during this period (Figure E2C). By contrast, sororin accumulation was greatly reduced in cells where Cdc5L and Prp19 were depleted (Figure 3A and E2A), when level of other known interphase cohesion factors was unaffected (Figure E2B). Similarly, reduced accumulation of sororin was also observed upon SF3a120 or U2AF65 depletion and SSA treatment (Figure 3B). These results indicate that splicing inactivation leads to reduced accumulation of sororin, possibly by perturbing the splicing of its pre-mRNA. Consistent with this possibility, increased retention of *sororin* RNA introns 1 and 2, as well as to a lesser extent that of intron 5 of *GUSB* RNA used as a control, could be observed in Prp19 and Cdc5L depleted cells when compared to control cells (Figure 3C). By contrast, no particular increased intron retention in *Smc1*, *Smc3*, *Scc1*, *SA1*, *SA2*, *Esco1* and *Esco2* could be observed (Figure E3D), indicating that *sororin* splicing was selectively affected by Prp19 complex inactivation. Similar observations were also made upon SF3a120 or U2AF65 depletion and SSA treatment (Figure 3D and E2F), although SSA had a stronger overall impact on RNA splicing. This indicates that Prp19 complex and spliceosome inactivation leads to accumulation of unspliced *sororin* pre-mRNA, and demonstrates that Prp19 complex is essential for the accumulation of sororin protein as a consequence of its function in splicing. This also suggest that the described

interaction between Prp19 complex and cohesin (McCracken et al., 2005), known to act in gene expression, could reflect a common function of these complexes in transcription regulation, RNA maturation, or in the coupling between these two processes.

Sororin is a protein conserved from fly to human that is degraded as cells exit from mitosis (Rankin and Kirschner, 2005) and accumulates during S phase (Nishiyama et al., 2010). If sororin reduction accounts for cohesion defects observed upon Prp19 complex inactivation, then this inactivation should produce phenotypes similar to those of sororin depletion. Consistent with this prediction, we observed that cohesin complexes were still associated with chromatin upon Cdc5L depletion (Figure E3E) indicating that Prp19 complex, similar to sororin (Schmitz et al., 2007), is dispensable for the association of cohesin with chromatin. Next we assessed interphase SCC by DNA fluorescence *in situ* hybridisation (FISH) using a probe recognising a region that is trisomic in HeLa cells (Figure 3E)(Schmitz et al., 2007; Watrin and Peters, 2006). We addressed cohesion status in cells depleted of Cdc5L, Prp19 or Scc1 by measuring distances between paired dots (Figure 3F). In control cells, the mean distance between paired FISH signals was 0.4  $\mu\text{m}$  and increased to 0.67  $\mu\text{m}$  in Scc1 depleted cells, and to 0.64  $\mu\text{m}$  and 0.65  $\mu\text{m}$  in Cdc5L and Prp19 depleted cells, respectively. Thus, similar to sororin, Prp19 complex is dispensable for cohesin loading onto chromatin and is required for interphase cohesion.

### **Correction of endogenous sororin protein level counteracts SCC deficiency caused by Prp19 complex inactivation**

These observations altogether strongly suggest that reduction in sororin protein accounts for defective cohesion caused by Prp19 inactivation. This implies that

correcting sororin protein level should rescue the cohesion defects caused by Prp19 complex inactivation. To test this prediction directly we generated an intron-free sororin coding sequence, expression of which in cells does not depend on splicing. We used this sequence to establish a cell line expressing sororin in fusion with GFP (sororin-GFP), which is expressed at a level close to that of endogenous sororin, and is resistant to siRNAs (Figure 4A). Both cell lines were treated with control, sororin, Scc1, Cdc5L and Prp19 siRNAs, and mitotic chromosome spreads were prepared and analysed at different times after transfection. As shown in Figure 4B, the proportion of wildtype cells exhibiting defective cohesion upon sororin depletion reached 84 % 48 hours after siRNA transfection. In sororin-GFP cells, this number was reduced to 44 %, indicating that sororin-GFP compensates partially for endogenous sororin depletion. This incomplete rescue might be due to uneven expression levels between cells or to sororin not being fully functional when tagged with GFP. By contrast, the expression of sororin-GFP had no effect on defective cohesion observed after Scc1 depletion (Figure 4B, upper panel) indicating that sororin-GFP only rescues cohesion defects caused by reduced sororin level. Finally, proportions of cells exhibiting defective cohesion upon Cdc5L and Prp19 depletion reached 84 % and 68 % respectively in wildtype cells, and decreased to 51 % and 46 % in sororin-GFP cells (Figure 4B, lower panel). These results indicate that expression of sororin-GFP is sufficient to rescue Cdc5L and Prp19 depletions, at least partly. This strongly supports the possibility that defective cohesion caused by inactivation of Prp19 complex directly originated from reduced level of sororin protein, although we cannot rule out that reduced level of another, as yet unidentified, cohesion factor could also participate in this phenotype. We also observed that, even though ectopic expression of sororin was able to correct defective SCC caused by

Prp19 complex inactivation, most mitotic cells in which cohesion had been restored still displayed abnormal spindles (unpublished observation, EW). Consequently, number of mitotic cells was similarly high in both cell lines upon Prp19 complex inactivation (Figure 4C). This indicates that sororin reduction, and therefore defective cohesion, is not the sole consequence of Prp19 complex inactivation, and suggests that Prp19 complex, or spliceosome activity, also impacts on proper assembly of mitotic spindle, in agreement with previous report (Hofmann et al., 2013). This observation also illustrates pleiotropic involvements of spliceosome in cell's progression through mitosis.

Finally, we took advantage of the anti-cohesive property of the protein Wapl. RNAi-mediated depletion of Wapl is able to rescue defective cohesion caused by sororin depletion (Nishiyama et al., 2010). Thus, if defective cohesion observed upon inactivation of Prp19 complex was caused by a reduction in sororin level, depleting Wapl at the same time should then restore normal SCC. To test this prediction, cells treated with control, sororin, Cdc5L and Prp19 siRNAs were eventually depleted of Wapl by RNAi (Figure 4D), and SCC was assessed by chromosome spreading. As shown before (Kueng et al., 2006), Wapl depletion prevented opening of chromosome arms in more than 80 % of prometaphase cells. Furthermore, the proportion of prometaphase cells exhibiting uncohered sister chromatid upon sororin depletion was reduced from 90 % to 12 % by the co-depletion of Wapl, as previously reported (Nishiyama et al., 2010). Finally, Wapl depletion was also able to rescue cohesion defects caused by Cdc5L and Prp19 depletions, further supporting the notion that cohesion defects originated from reduced level of sororin. Altogether these results indicate that reduced expression of sororin consequent to defective splicing of its pre-mRNA accounts for defective cohesion upon Prp19 complex

inactivation. Why would *sororin* pre-mRNA be so sensitive to splicing inactivation? In contrast to other known interphase cohesion factors, present at similar cellular level throughout the cell cycle, *sororin* is degraded at every cell's exit from mitosis. Hence, robust SCC relies on *de novo* production of *sororin* proteins during S phase, and would thus be particularly sensitive to defective processing of *sororin* pre-mRNA, as compared to that of pre-mRNAs encoding other cohesion factors. In addition, we showed that splicing of *sororin* was more sensitive to spliceosome inactivation than any other well established interphase cohesion factors, although the molecular basis for this difference remains to be determined.

Interestingly, genome-wide RNAi studies have shown that depletion of 30 distinct splicing factors, including factors studied here, resulted in perturbed mitosis (Hofmann et al., 2010; Neumann et al., 2010), consistent with defective SCC. Mark Petronczki and his collaborators made the striking discovery that depletion of any of these 30 splicing factors resulted in defective cohesion in mitosis (personal communication), identical to results we reported here, indicating that inactivation of various splicing factors causes remarkably similar SCC defects and strongly suggesting that defective cohesion, possibly due to reduced level of *sororin*, is a common feature of altered splicing machinery. Mutations in SCC apparatus genes are associated with cancers, including myeloid neoplasms (Kon et al., 2013), bladder cancer (Balbas-Martinez et al., 2013), glioblastoma, melanoma and Ewing's sarcoma (Solomon et al., 2011) and trigger aneuploidy and chromosome instability in glioblastoma cells (Solomon et al., 2011). Recent work has suggested that acquisition of mutations in SCC components is an important step in oncogenic process (Yoshida et al., 2013). Similarly, mutations in genes encoding splicing factors are also found in cancers such as myeloid neoplastic disorders (Yoshida et al.,

2011) and chronic lymphocytic leukaemia (Ebert and Bernard, 2011). Based on our findings that perturbation of the splicing machinery alters cohesin and SCC regulation, it is possible that deleterious mutations in splicing genes participate in oncogenesis by promoting genome instability through defective cohesin functions, at least in some cancer types. Further molecular investigations in different cancers will be essential to determine if and how splicing machinery deficiencies participate in tumourisation through defective cohesion.

## **Experimental procedures**

### **RNA extraction, reverse transcription, PCR and quantitative PCR analyses**

Total RNAs were extracted from HeLa cells using the RNeasy kit (Qiagen). 1 µg of total RNAs served as matrix in reverse transcription reaction using Superscript II reverse transcriptase (Life Technologies). PCR reactions were performed using primer pairs that specifically span from exon 2 to exon 3 of p80-coilin pre-mRNA or amplify the junction between exon 3 (e3) and intron 3 (i3) of β-actin pre-mRNA (sequences were described in (Kaida et al., 2007; Tanackovic and Kramer, 2005), respectively). PCR products were analysed by electrophoresis on 1 % agarose gel. Quantitative real time PCR analyses were performed using Power-Sybr mix on a 7700 QPCR ABI following the manufacturer's instructions with primers shown in Table E1. For intron retention, the relative abundance of pre-mRNA over total RNA (pre-mRNA+mRNA) was calculated as follows:  $-\Delta Ct = -(Ct_{\text{pre-mRNA}} - Ct_{\text{total RNA}})$ . The relative abundance of total RNAs was calculated as:  $-\Delta Ct = -(Ct_{\text{exon}} - Ct_{\text{exonGUSB}})$ . All measures were done in triplicates. Intron-spanning primer pairs were used for mature mRNAs, primers amplifying exon-intron or intron-exon junctions were used for pre-mRNAs, and pairs within one exon were used for total RNAs (Table E1).

### **Cell culture, synchronisation and RNAi**

HeLa cells were grown in DMEM (Invitrogen) supplemented with 10 % foetal bovine serum (PAA), 0.2 mM L-glutamine and antibiotics (Invitrogen). Single mCdc5L-LAP cell clones were isolated from an mCdc5L-LAP cell pool, selected in medium containing 800 µg/ml geneticin (PAA) and maintained in medium supplemented with 400 µg/ml geneticin. Sororin-GFP cell lines were obtained by transfection and subsequent selection with 800 µg/ml of geneticin (Invitrogen) and were maintained in

the presence of 200 µg/ml of geneticin. For double-thymidine arrest synchronisation procedure, cells were treated for 24 hours with 2 mM thymidine, washed twice with 37°C PBS and released in fresh complete medium. 6 hours later, thymidine was added for 18 hours. Synthetic siRNA oligonucleotides were purchased from Ambion and Eurogentec, and were used at a final concentration of 100 nM to transfect cells in the presence of Jetprime (PolyPlus Transfection). The sequences of the control, Scc1, Wapl and sororin siRNAs used here have been described elsewhere (Kueng et al., 2006; Schmitz et al., 2007; Watrin et al., 2006). The sequences of Cdc5L, Prp19 and SF3a120 have also been described in previous studies (Liu et al., 2009; Tanackovic and Kramer, 2005). Sequence of U2AF65 siRNA used in this study was: 5'-AAGGUCCGUAAAU-ACUGGGACdTdT-3'. Cells were used at the indicated times after transfection. The small inhibitor spliceostatin A was kindly provided by Minoru Yoshida (Kaida et al., 2007).

### **Immunofluorescence and chromosome spreads**

Immunofluorescence staining, was performed as previously described (Watrin and Legagneux, 2005). Immunofluorescence analyses were performed using a fluorescent microscope (DMRXA2 Leica) with a 40x oil immersion objective lens, and images were processed using MetaMorph software (Molecular Devices). For chromosome spread, cells were treated for 30 minutes with 100 ng/mL of nocodazole. Cells were collected and resuspended in 1 mL of medium, 1.5 mL of tap water was added. 6 minutes later 7 mL of Carnoy fixative (3:1, methanol: glacial acetic acid). Cells were then spreads on glass slide, dried, stained with Giemsa stain and mounted in Entellan. Mitotic chromosome spreads observations were made using a light microscope (DM2000 Leica) with a 40x dry objective.

## **Expanded view inventory**

Figure E1. Additional materials in support to Figure 1.

Figure E2. Additional materials in support to Figure 3.

Table E1. List of primers used in real-time quantitative PCR, related to Figure 3.

Expanded view figure legends.

## **Acknowledgements**

We would like to thank Angela Krämer, Laura Magnani-Jaulin and Jan-Michael Peters for antibodies and Minoru Yoshida for spliceostatin A. We also thank Ina Poser and Tony Hyman for mCdc5L-LAP cell pools, members of Luc Paillard's lab for advice on qPCR, and MRiC facility. We are grateful to Christian Jaulin and Vincent Legagneux for comments on the manuscript, and also to Mark Petronczki for discussion and for sharing unpublished data. This work was supported in part by grants to EW from Rennes Métropole, the Institut National du Cancer (INCa, PLBIO2012), the Région Bretagne and the European ERA-Net via the "Rare Disease" (E-Rare 2, TARGET-CdLS) program and the French Agence Nationale de la Recherche (ANR).

## References

- Ajuh P, Kuster B, Panov K, Zomerdijk JC, Mann M and Lamond AI. (2000) Functional analysis of the human CDC5L complex and identification of its components by mass spectrometry. *Embo J*, **19**, 6569-6581.
- Balbas-Martinez C, Sagrera A, Carrillo-de-Santa-Pau E, Earl J, Marquez M, Vazquez M, Lapi E, Castro-Giner F, Beltran S, Bayes M, et al. (2013) Recurrent inactivation of STAG2 in bladder cancer is not associated with aneuploidy. *Nat Genet*, **45**, 1464-1469.
- Chanarat S, Seizl M and Strasser K. (2011) The Prp19 complex is a novel transcription elongation factor required for TREX occupancy at transcribed genes. *Genes Dev*, **25**, 1147-1158.
- Cheng SC, Tarn WY, Tsao TY and Abelson J. (1993) PRP19: a novel spliceosomal component. *Mol Cell Biol*, **13**, 1876-1882.
- Ebert, B. and Bernard, O.A. (2011) Mutations in RNA splicing machinery in human cancers. *N Engl J Med*, **365**, 2534-2535.
- Gandhi R, Gillespie PJ and Hirano T. (2006) Human Wapl is a cohesin-binding protein that promotes sister-chromatid resolution in mitotic prophase. *Curr Biol.*, **16**, 2406-2417. Epub 2006 Nov 2416.
- Grote M, Wolf E, Will CL, Lemm I, Agafonov DE, Schomburg A, Fischle W, Urlaub H and Luhrmann R. (2010) Molecular architecture of the human Prp19/CDC5L complex. *Mol Cell Biol*, **30**, 2105-2119.
- Guacci V, Koshland D and Strunnikov A. (1997) A direct link between sister chromatid cohesion and chromosome condensation revealed through the analysis of MCD1 in *S. cerevisiae*. *Cell*, **91**, 47-57.
- Hoffman BE and Grabowski PJ. (1992) U1 snRNP targets an essential splicing factor, U2AF65, to the 3' splice site by a network of interactions spanning the exon. *Genes Dev.*, **6**, 2554-2568.
- Hofmann JC, Husedzinovic A and Gruss OJ. (2010) The function of spliceosome components in open mitosis. *Nucleus.*, **1**, 447-459.. Epub 12010 Aug 13313.
- Hofmann JC, Tegha-Dunghu J, Drager S, Will CL, Luhrmann R and Gruss OJ. (2013) The prp19 complex directly functions in mitotic spindle assembly. *PLoS One*, **8**, 0074851.
- Kaida D, Motoyoshi H, Tashiro E, Nojima T, Hagiwara M, Ishigami K, Watanabe H, Kitahara T, Yoshida T, Nakajima H, et al. (2007) Spliceostatin A targets SF3b and inhibits both splicing and nuclear retention of pre-mRNA. *Nat Chem Biol*, **3**, 576-583.

Kon A, Shih LY, Minamino M, Sanada M, Shiraishi Y, Nagata Y, Yoshida K, Okuno Y, Bando M, Nakato R, et al. (2013) Recurrent mutations in multiple components of the cohesin complex in myeloid neoplasms. *Nat Genet*, **45**, 1232-1237.

Kueng S, Hegemann B, Peters BH, Lipp JJ, Schleiffer A, Mechtler K and Peters JM. (2006) Wapl controls the dynamic association of cohesin with chromatin. *Cell.*, **127**, 955-967. Epub 2006 Nov 2016.

Losada A, Hirano M and Hirano T. (1998) Identification of Xenopus SMC protein complexes required for sister chromatid cohesion. *Genes Dev*, **12**, 1986-1997.

Losada A, Yokochi T and Hirano T. (2005) Functional contribution of Pds5 to cohesin-mediated cohesion in human cells and Xenopus egg extracts. *J Cell Sci*, **118**, 2133-2141. Epub 2005 Apr 2126.

Losada A, Yokochi T, Kobayashi R and Hirano T. (2000) Identification and Characterization of SA/Scp3p Subunits in the Xenopus and Human Cohesin Complexes. *J Cell Biol*, **150**, 405-416.

McCracken S, Longman D, Marcon E, Moens P, Downey M, Nickerson JA, Jessberger R, Wilde A, Caceres JF, Emili A, et al. (2005) Proteomic analysis of SRm160-containing complexes reveals a conserved association with cohesin. *J Biol Chem.*, **280**, 42227-42236. Epub 42005 Sep 42213.

Michaelis C, Ciosk R and Nasmyth K. (1997) Cohesins: chromosomal proteins that prevent premature separation of sister chromatids. *Cell*, **91**, 35-45.

Neumann B, Walter T, Heriche JK, Bulkescher J, Erfle H, Conrad C, Rogers P, Poser I, Held M, Liebel U, et al. (2010) Phenotypic profiling of the human genome by time-lapse microscopy reveals cell division genes. *Nature*, **464**, 721-727.

Nishiyama T, Ladurner R, Schmitz J, Kreidl E, Schleiffer A, Bhaskara V, Bando M, Shirahige K, Hyman AA, Mechtler K, et al. (2010) Sororin mediates sister chromatid cohesion by antagonizing Wapl. *Cell*, **143**, 737-749.

Ouyang Z, Zheng G, Song J, Borek DM, Otwinowski Z, Brautigam, CA, Tomchick DR, Rankin S and Yu H. (2013) Structure of the human cohesin inhibitor Wapl. *Proc Natl Acad Sci U S A*, **110**, 11355-11360.

Rankin S, Ayad NG and Kirschner MW. (2005) Sororin, a substrate of the anaphase-promoting complex, is required for sister chromatid cohesion in vertebrates. *Mol Cell*, **18**, 185-200.

Rolef Ben-Shahar T, Heeger S, Lehane C, East P, Flynn H, Skehel M and Uhlmann F. (2008) Eco1-dependent cohesin acetylation during establishment of sister chromatid cohesion. *Science*, **321**, 563-566.

Schmitz J, Watrin E, Lenart P, Mechtler K and Peters JM. (2007) Sororin is required for stable binding of cohesin to chromatin and for sister chromatid cohesion in interphase. *Curr Biol*, **17**, 630-636.

Solomon DA, Kim T, Diaz-Martinez LA, Fair J, Elkahloun AG, Harris BT, Toretsky JA, Rosenberg SA, Shukla N, Ladanyi M, et al. (2011) Mutational inactivation of STAG2 causes aneuploidy in human cancer. *Science*, **333**, 1039-1043.

Sumara I, Vorlaufer E, Gieffers C, Peters BH and Peters JM. (2000) Characterization of vertebrate cohesin complexes and their regulation in prophase. *J Cell Biol*, **151**, 749-762.

Tanackovic G and Kramer A. (2005) Human splicing factor SF3a, but not SF1, is essential for pre-mRNA splicing in vivo. *Mol Biol Cell*, **16**, 1366-1377.

Tarn WY, Lee KR and Cheng SC. (1993) The yeast PRP19 protein is not tightly associated with small nuclear RNAs, but appears to associate with the spliceosome after binding of U2 to the pre-mRNA and prior to formation of the functional spliceosome. *Mol Cell Biol*, **13**, 1883-1891.

Unal E, Heidinger-Pauli JM, Kim W, Guacci V, Onn I, Gygi SP and Koshland DE. (2008) A molecular determinant for the establishment of sister chromatid cohesion. *Science*, **321**, 566-569.

Watrin E and Peters JM. (2006) Cohesin and DNA damage repair. *Exp Cell Res.*, **312**, 2687-2693. Epub 2006 Jun 2622.

Yoshida K, Sanada M, Shiraishi Y, Nowak D, Nagata Y, Yamamoto R, Sato Y, Sato-Otsubo A, Kon A, Nagasaki M, et al. (2011) Frequent pathway mutations of splicing machinery in myelodysplasia. *Nature*, **478**, 64-69.

Yoshida K, Toki T, Okuno Y, Kanezaki R, Shiraishi Y, Sato-Otsubo A, Sanada M, Park MJ, Terui K, Suzuki H, et al. (2013) The landscape of somatic mutations in Down syndrome-related myeloid disorders. *Nat Genet*, **45**, 1293-1299.

Zhang J, Shi X, Li Y, Kim BJ, Jia J, Huang Z, Yang T, Fu X, Jung SY, Wang Y, et al. (2008) Acetylation of Smc3 by Eco1 is required for S phase sister chromatid cohesion in both human and yeast. *Mol Cell*, **31**, 143-151.

Zhang N, Kaur R, Akhter S and Legerski RJ. (2009) Cdc5L interacts with ATR and is required for the S-phase cell-cycle checkpoint. *EMBO Rep*, **10**, 1029-1035.

## Figure legends

Figure 1. Depletion of either Cdc5L or Prp19 causes precocious sister chromatid separation in mitosis and arrests cells in a prometaphase-like state.

(A-D) Wildtype and mCdc5L-LAP HeLa cells were transfected with control, Scc1, Cdc5L and Prp19 siRNAs and chromosome spreads were prepared 24, 48 and 72 hours after transfection. (A) Representative images of chromosome spreads. The percentages of phenotypes for wildtype and for mCdc5L-LAP HeLa prometaphase cells are shown in (B) and (C), respectively (n > 100 per condition). (D) Depletion efficiency was analysed by immunoblotting with the antibodies indicated 72 hours after transfection.

(E) Aurora B remains at the centromere in Cdc5L, Prp19 or Scc1 depleted cells. Cells transfected as in (A) were fixed and stained with human CREST serum (red) and Aurora B antibody (green). DNA (blue) was stained with DAPI.

Figure 2. Depletion of the splicing factors SF3a120 and U2AF65 or chemical inhibition of the splicing machinery cause premature separation of sister chromatids in mitosis.

(A-B) HeLa cells were transfected with control and SF3a120 (A) or U2AF65 (B) siRNAs, and chromosome spreads were prepared 24 and 48 hours after transfection. Percentages of prometaphase cells displaying defective cohesion were determined (middle panels, n > 100 per condition). Depletion efficiency was analysed by immunoblotting with the antibodies indicated (left panels). Percentages of prometaphase cells in each condition are shown in right panels.

(C) HeLa cells were treated with 5 nM of SSA or with methanol for 24 hours. RT-PCR reaction were performed to detect intron retention in *p80-coilin* and *β-actin* pre-

mRNAs and analysed on agarose gel (left panels). In parallel, cells were left untreated or treated for 24 hours with methanol, 0.5 or 2 nM of SSA and processed as in (A). Percentages of prometaphase cells displaying defective cohesion are shown (middle panel,  $n > 100$  per condition), and percentages of prometaphase cells are shown in right panel.

Figure 3. Inactivation of Prp19 complex impairs sororin protein accumulation and triggers defective cohesion in postreplicative interphase cells.

(A) HeLa cells were transfected with control, Cdc5L (left panel) or Prp19 (right panel) siRNAs and synchronised by double thymidine block procedure. 72 hours after transfection, total cell extracts were prepared before (0 h) or 4 hours after the second release (4 h) and analysed by immunoblotting using the antibodies indicated.

(B) HeLa cells were transfected with control, SF3a120 (left panel) or U2AF65 (middle panel) siRNAs and synchronised by double thymidine block procedure. 72 hours after transfection, total cell extracts were prepared and analysed as in (A). Synchronised cells treated for 24 hours with spliceostatin A were collected before (0 h) or 4 hours following the second release (4h), and were analysed as in (A) (right panel).

(C) Total RNAs were extracted from control, Cdc5L and Prp19 depleted cells, and real-time quantitative PCR experiments were performed to determine the abundances of pre-mRNA for *sororin* and for *GUSB* (used as a control) in the different RNAi conditions. Results are expressed as  $-\Delta\text{Ct}$  (log scale) relative to those obtained for total RNA using primer pairs specific for *sororin* exon 5 and *GUSB* exon 7. Results of four independent experiments are presented (mean  $\pm$  SEM).

(D) Total RNAs were extracted from control, SF3A120, U2AF65 depleted and cells treated with SSA, and the abundances of pre-mRNA for *sororin* and for *GUSB* were

analysed as in (C). Results of three independent experiments are presented (mean  $\pm$  SEM).

(E-F) DNA FISH of control, Scc1, Cdc5L and Prp19 depleted G2 cells. (E) Representative images of DAPI-stained nuclei (blue) with paired FISH signals (red) are shown. Insets show magnified images of single FISH signal pairs. (F) Quantification of distances between paired FISH signals obtained in the experiment described in (E) (mean  $\pm$  SD;  $n \geq 30$  per condition). Asterisks indicate a significant difference to the control in Student's *t* test ( $p < 0.01$ ).

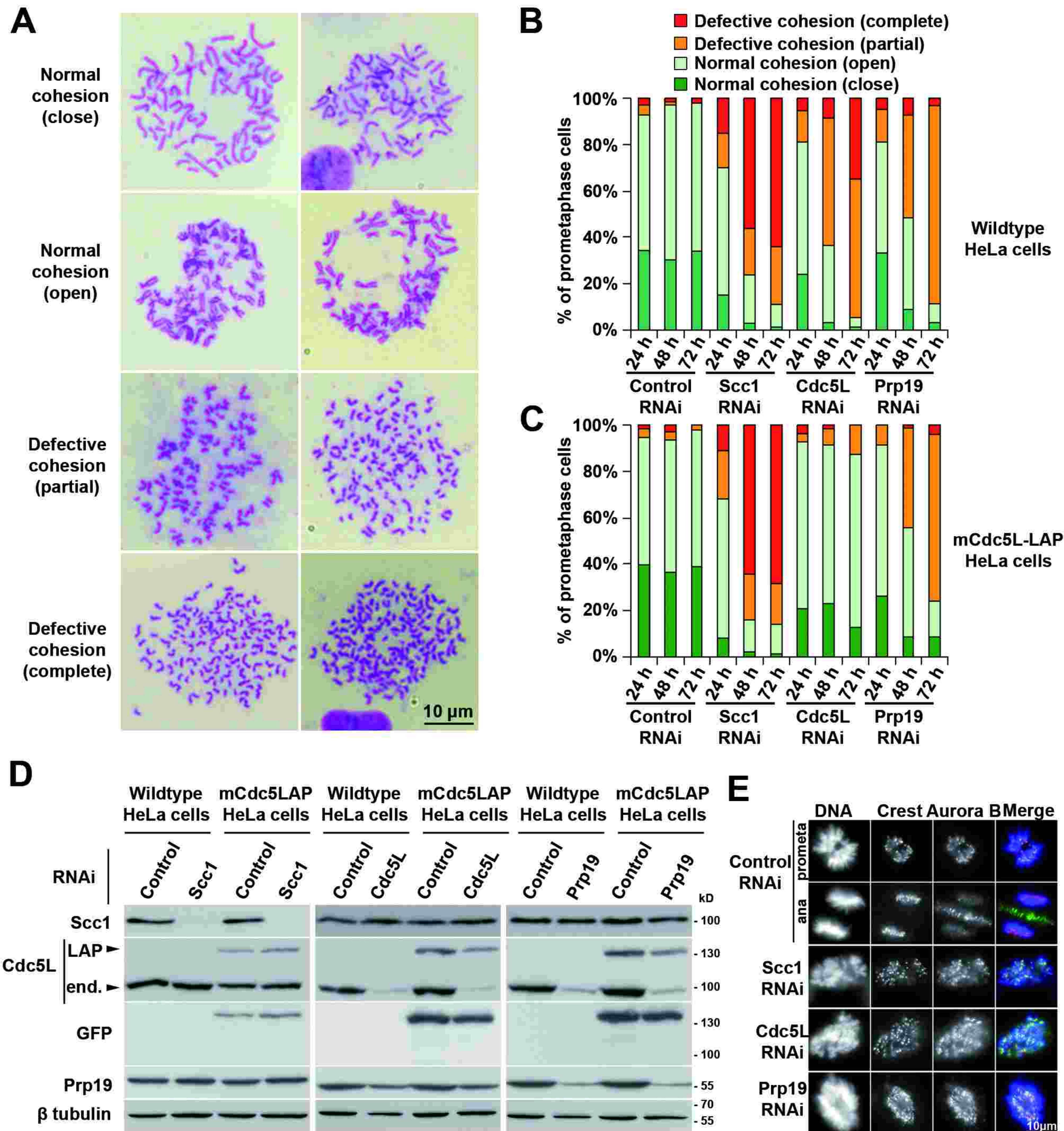
Figure 4. Ectopic correction of sororin protein level and depletion of Wapl rescue cohesion deficiency caused by Prp19 complex inactivation.

(A) Wildtype and sororin-GFP HeLa cells were transfected with control and sororin siRNAs. 48 hours after transfection, total cell extracts were prepared and analysed by immunoblotting experiments using the antibodies indicated.

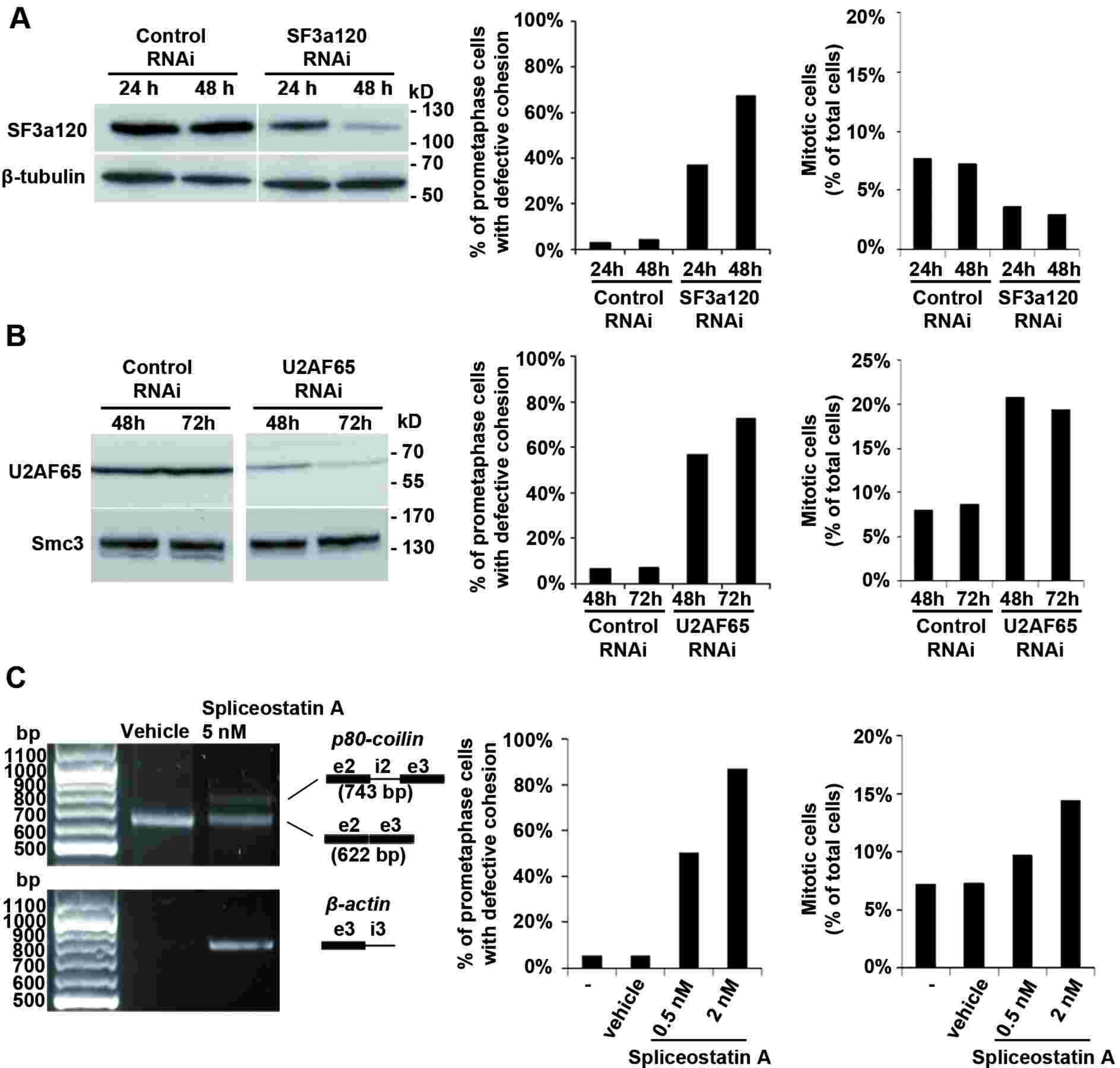
(B-C) Wildtype and sororin-GFP HeLa cells were transfected with control, Sororin, Scc1, Cdc5L and Prp19 siRNAs. At the indicated time after transfection, chromosome spreads were prepared as described. Percentages of prometaphase cells displaying defective cohesion as defined in Figure 1 are shown in panel (B) ( $n > 100$  per condition), and corresponding mitotic indices are shown in (C) ( $n > 300$  per condition).

(D) HeLa cells transfected (+) or not (-) with Wapl siRNAs were also transfected with control, sororin, Cdc5L and Prp19 siRNAs, and mitotic chromosome spreads were prepared 48 and 72 hours later. Percentages of prometaphase cells that exhibit close or open chromosome conformation (normal cohesion) and defective cohesion, as defined in Figure 1A, are shown ( $n > 100$  per condition).





**Figure 2**



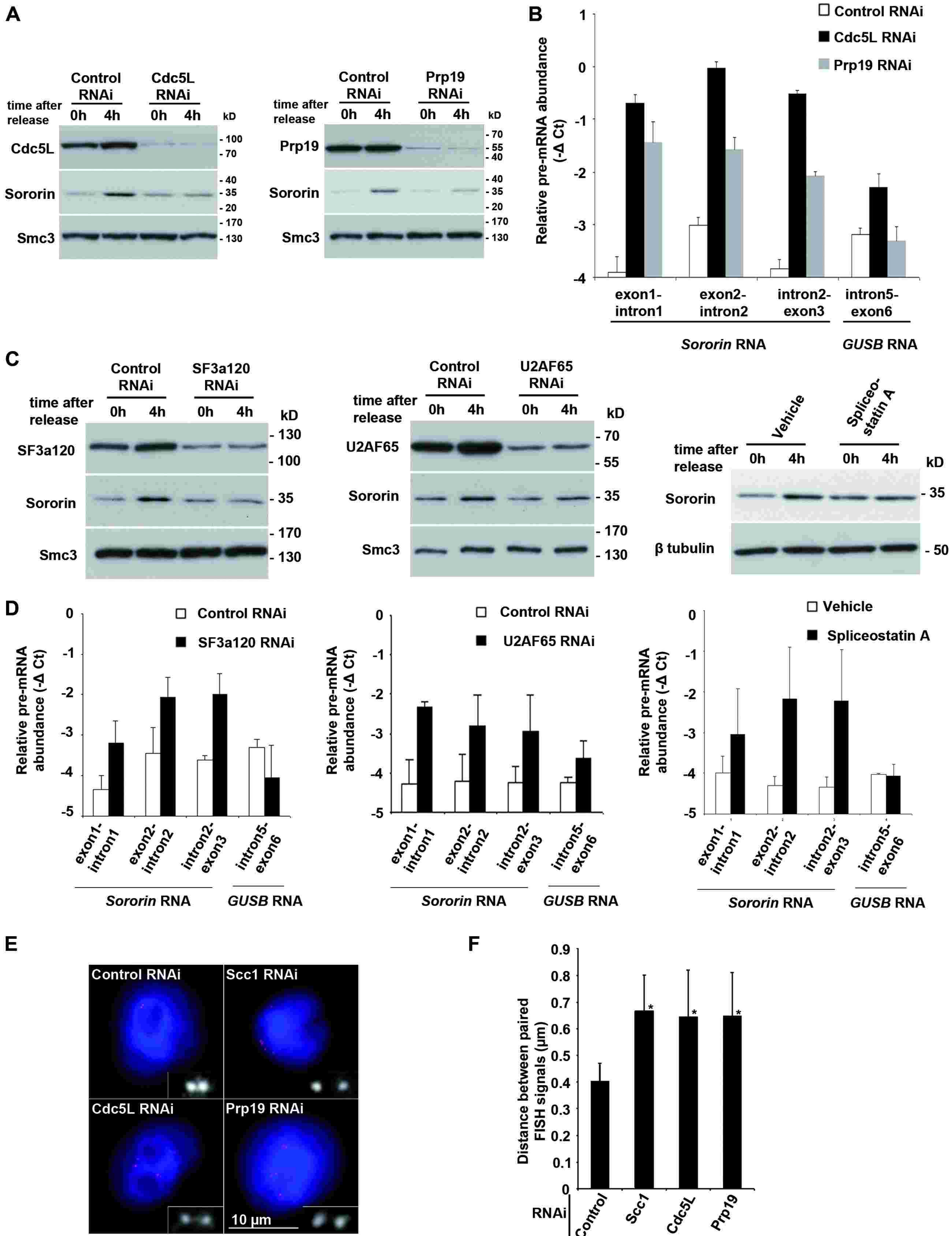
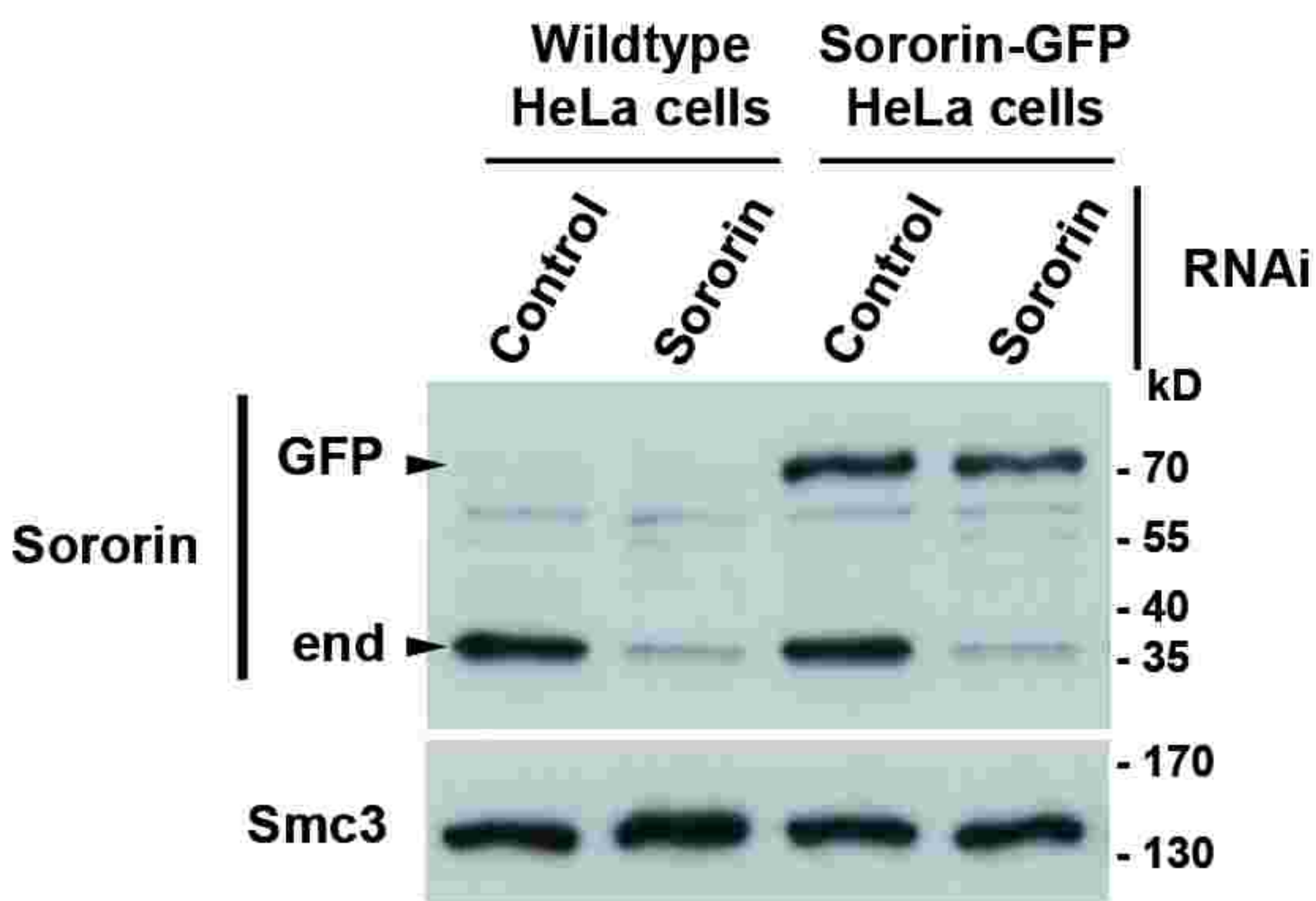
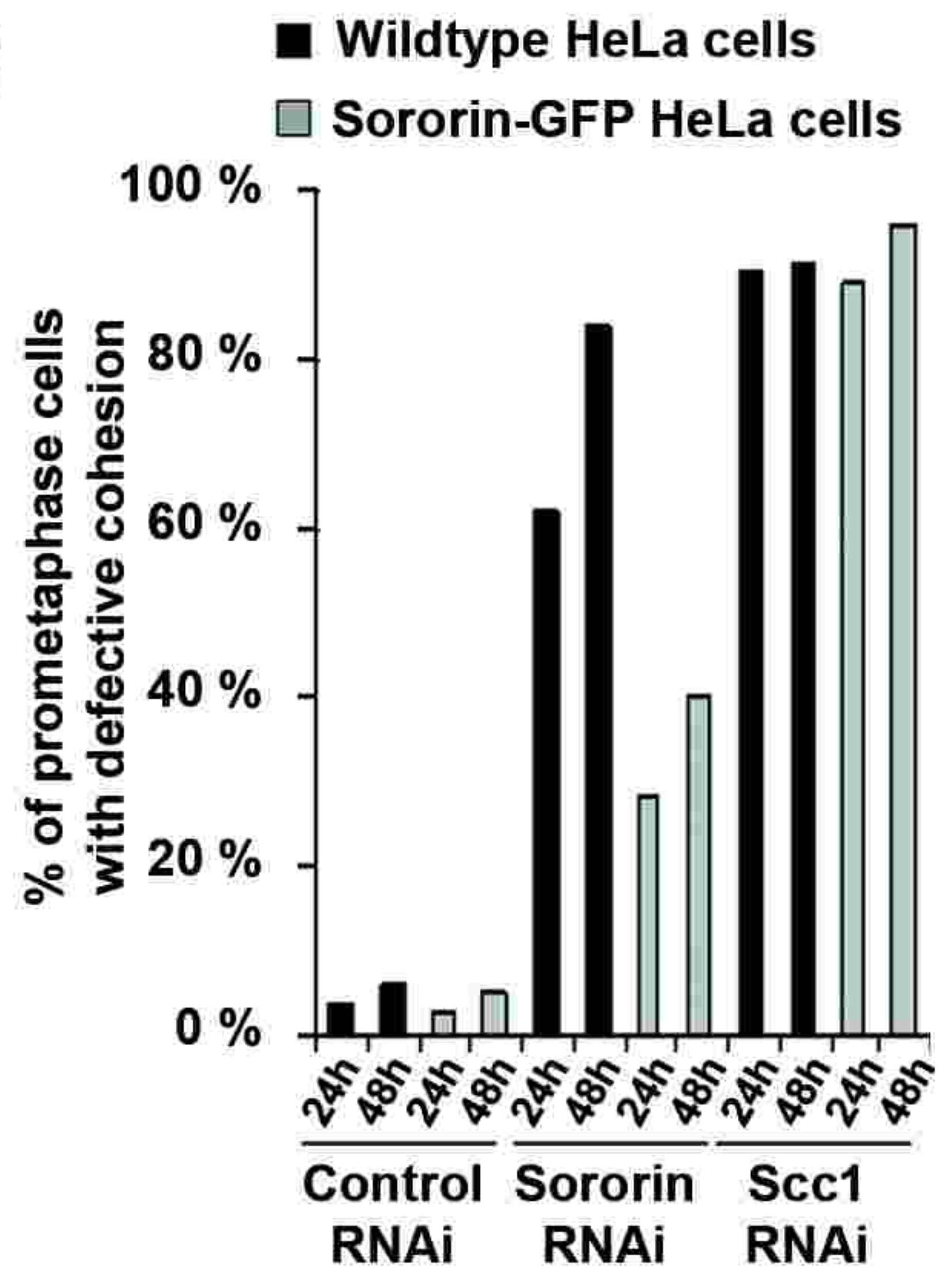


# Figure 4

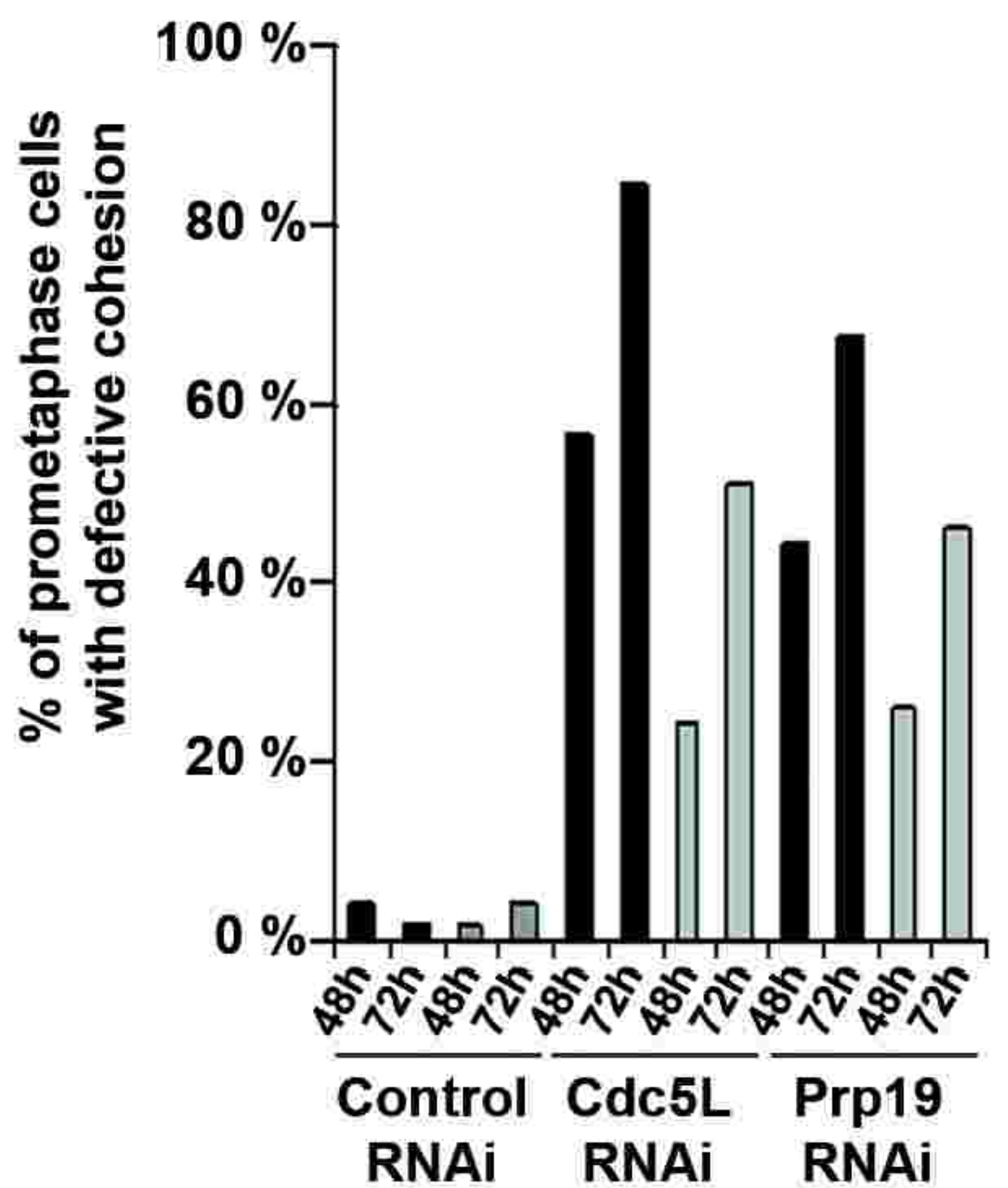
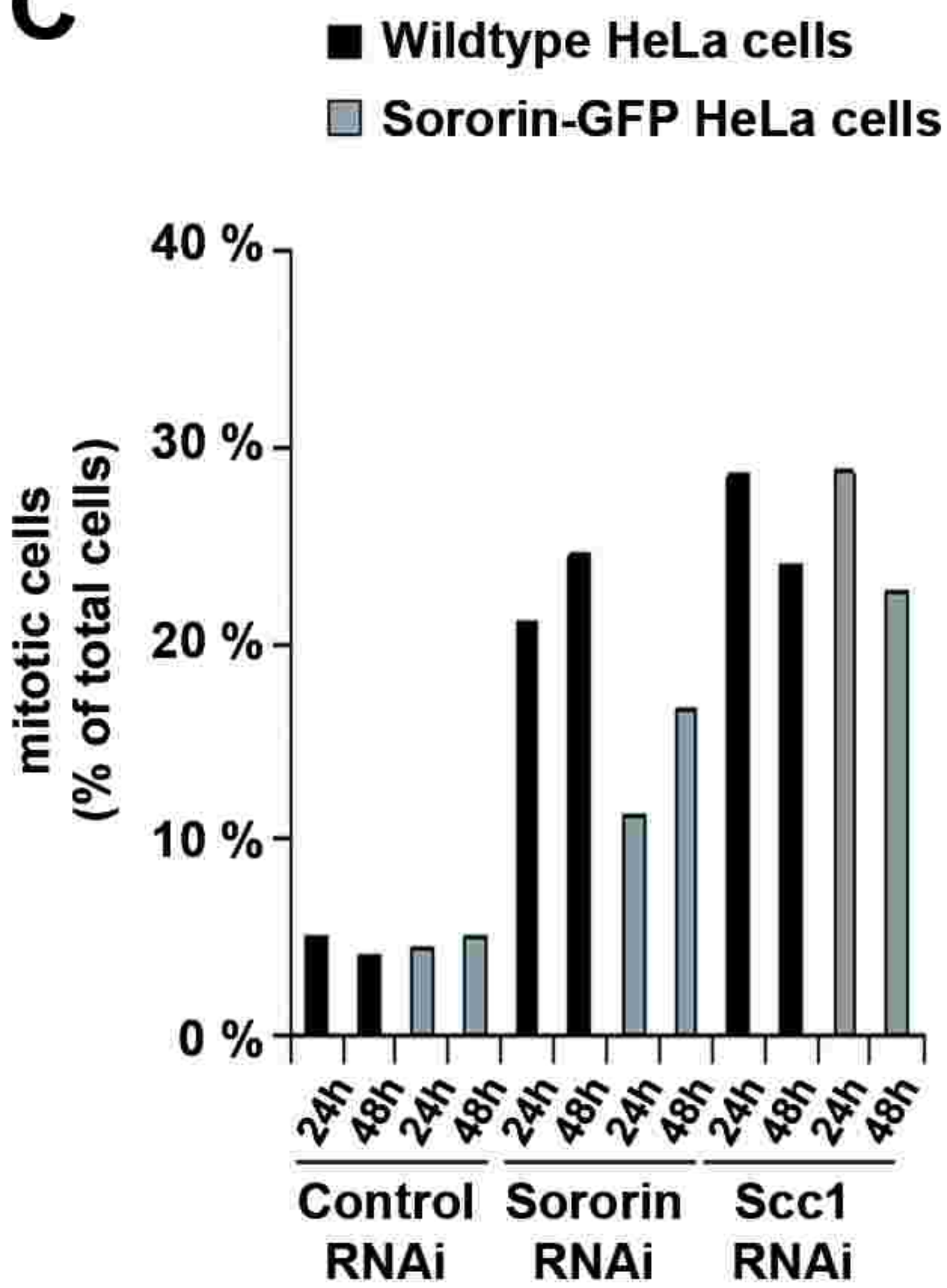
## A



## B



## C



## D

